Proceedings World Geothermal Congress 2026
Calgary, Canada, June 8 – 11, 2026

Evolution of Fractured Carbonate Reservoirs: Understanding Physical and Chemical Responses to Reinjection in the Menderes Massif, Türkiye

Taygun Uzelli[1,2], Shannon L. Flynn[2], Cees van der Land[2], Sanem Acikalin[2], Stuart Jones[3]

[1]Geothermal Energy Research and Application Center, Izmir Institute of Technology, İzmir, Türkiye

[2]School of Natural and Environmental Sciences, Newcastle University, Newcastle, UK

[3]Department of Earth Sciences, Durham University, Durham, UK

*taygunuzelli@iyte.edu.tr

Keywords: Menderes Massif, fluid reinjection, fracture permeability, physicochemical interactions, geothermal reservoir.

1 INTRODUCTION

Geothermal energy is a key pillar of the global clean energy transition, providing reliable baseload power independent of seasonal or climatic variability. Türkiye ranks among the world's leading producers, largely due to the rapid development of high-enthalpy geothermal fields in Western Anatolia, where deep, naturally fractured reservoirs sustain electricity generation. Maintaining long-term productivity in these systems depends on balancing extraction with reinjection: cooler, CO_2-enriched fluids are returned to the subsurface to preserve reservoir pressure, but this process simultaneously triggers complex thermal, hydraulic, and geochemical feedbacks. Fractured carbonate reservoirs are especially sensitive to these perturbations. Reinjection can disrupt fluid–rock equilibrium, alter fracture connectivity, and induce mineral dissolution or precipitation, which affects porosity, permeability, and injectivity. However, key subsurface processes remain poorly constrained, as most monitoring emphasizes wellhead pressure–temperature data rather than in-reservoir evolution. In heterogeneous metamorphosed carbonate systems, where flow is governed by fracture networks rather than matrix porosity, temperature–pressure fluctuations, repeated reinjection cycles, and CO_2 enrichment can significantly modify mineral stability, potentially reducing injectivity or narrowing fracture apertures through precipitation of carbonate or silica phases.

To advance understanding of these reservoir responses, this study integrates experimental and analytical approaches to investigate the physicochemical evolution of carbonate–schist lithologies representative of Western Türkiye's geothermal systems. Controlled hydrothermal experiments conducted at Newcastle and Durham Universities simulate realistic reservoir conditions across varying temperatures (25-50-70-110°C), pressures, and CO_2-rich fluid compositions. These experiments are paired with multi-method post-reactive analyses, including XRD, XRF, SEM, ICP-OES, and high-resolution micro-CT, which allow for the detailed characterization of mineralogical transformations, porosity–permeability changes, and microstructural alterations that traditional methods cannot resolve. Through this combined workflow, the research aims to generate a more process-based understanding of how geothermal reservoirs evolve under coupled thermal–hydraulic–chemical (THC) conditions, ultimately supporting the development of more resilient and sustainable geothermal fields.

2 STUDY AREA AND GEOLOGICAL FRAMEWORK

The study area lies within the actively extending Aegean extensional domain, where the Gediz–Alaşehir Graben forms one of Türkiye's most prominent geothermal corridors (Figure 1). This NW–SE–trending half-graben system developed on the metamorphic Menderes Massif basement and is overlain by Neogene basin-fill sediments (İztan and Yazman, 1990; Çiftçi and Bozkurt, 2009). Regional tectonic evolution is governed by large-scale Miocene–recent crustal extension, in which low-angle normal faulting along the Gediz detachment played a central role in footwall exhumation, back-tilted stratigraphy, and the development of extensional folding along the southern margin (Koçyiğit et al., 1999; Sözbilir, 2001; Bozkurt and Sözbilir, 2004).

The Menderes Massif, forming the metamorphic basement of major geothermal provinces across Western Türkiye, consists predominantly of marble, schist, quartzite, and gneiss. These units have undergone multiple deformation phases, resulting in foliation, recrystallization, and fracture development that collectively enhance secondary porosity. Within this framework, the Gediz Graben hosts some of the country's most productive high-enthalpy geothermal fields, particularly in the Alaşehir–Salihli sector. Reservoirs are dominated by fractured and locally recrystallized carbonate units (limestones, dolomites, and marbles) interlayered with schist horizons that can significantly contribute to reservoir storage and injectivity due to their fracture susceptibility and

deformability. High-angle normal faults, transfer zones, and fracture corridors associated with N–S extension further enhance permeability, enabling geothermal fluids to circulate along structurally controlled pathways.

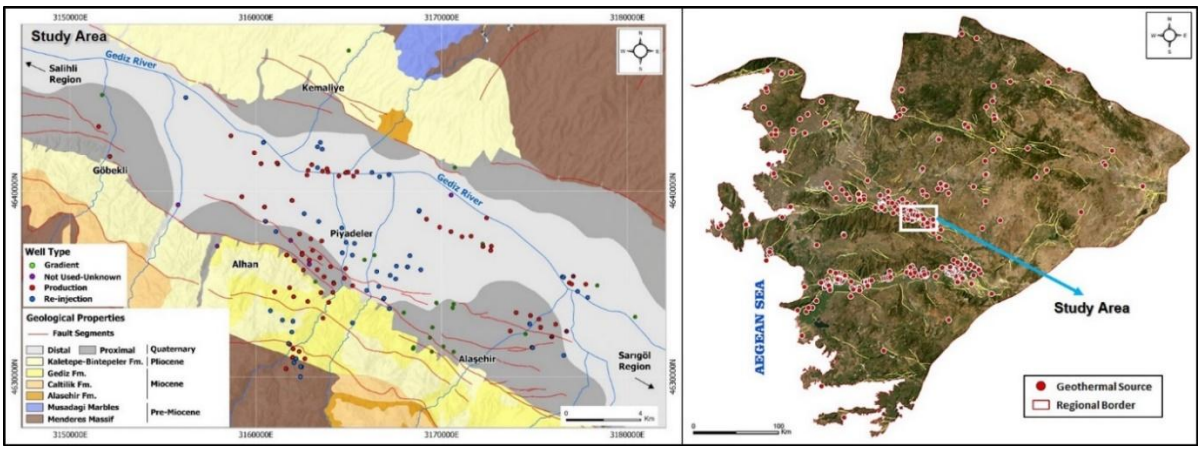


Figure 1. Location map and geological units of the study area (modified after Akbaş et al., 2011; DSI, 2014; Emre et al., 2018; Stantec, 2020)

3 METHODS & RESULTS

3.1 Reservoir Rock Characterization

Integrated petrographic, micro-CT, well-based, and outcrop-scale observations show that both carbonate- and schist-dominated intervals of the Menderes Massif effectively host geothermal fluids, with permeability controlled predominantly by fracture intensity, foliation planes, and structural fabrics rather than primary matrix porosity. Thin-section analyses reveal a heterogeneous and anisotropic porosity–permeability architecture shaped by depositional microfacies and metamorphic overprinting. Marble–schist alternations exhibit limited primary porosity; however, foliation-parallel microfractures form the dominant fluid pathways, consistent with mud-loss records from drilling. Grain-supported microfacies (grainstone, packstone) exhibit well-connected interparticle pores, whereas mudstones and recrystallized marbles depend heavily on fracture-related permeability. High-resolution micro-CT imaging of schist samples reveals matrix porosities ranging from 0.10% to 0.36%, which approach values observed in carbonate units and are significantly higher than expected for metamorphic schists enhanced with secondary permeability. Their internal fabric, defined by schistosity, aligned mica-rich foliation planes, and deformation-induced microcracks, creates a meaningful pore network and, more importantly, enhances permeability by providing preferential fluid pathways along mechanically weakened foliation surfaces. This finding challenges the conventional view that schist intervals contribute minimally to reservoir performance, instead demonstrating that schist-dominated horizons can play a critical role in both fluid storage and production. Thin-section images (Figure 2) further corroborate these interpretations: fossil-bearing carbonates, cross-cutting fracture networks, and blue-dye-highlighted pore structures directly illustrate how fractures and foliation-related microvoids dominate the effective flow pathways. The presence of interconnected pore domains in both carbonate and schist samples visually confirms the mixed fracture–matrix system inferred from micro-CT and well data. Collectively, these results indicate that reservoir quality in the Menderes Massif is governed by the interplay between facies-dependent pore structures, foliation- and fracture-controlled permeability, microfracturing intensity, and dissolution-enhanced porosity, underscoring the importance of integrating digital and classical methods when evaluating geothermal reservoirs in structurally complex metamorphic terrains.

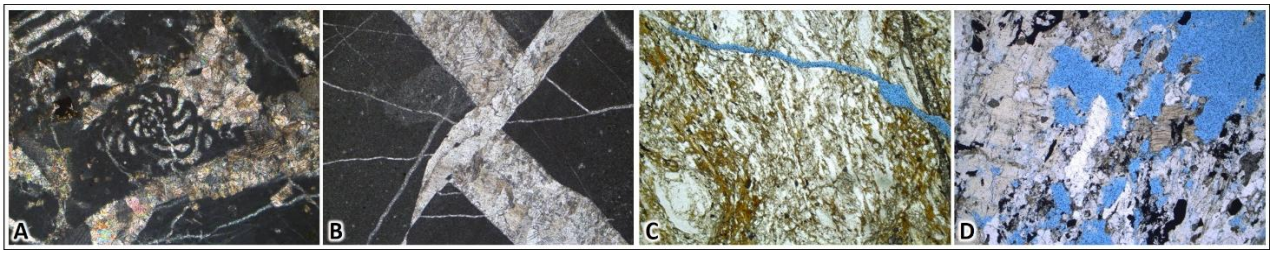


Figure 2. Representative thin-section photomicrographs from the reservoir rocks. a) Fossiliferous textures with bioclastic components preserved within the carbonate matrix. b) Microtectonic features showing cross-cutting calcite-filled veins and deformation bands. c) Fracture plane highlighted by blue-dye impregnation, revealing open fracture apertures and limited mineral infill. d) Intergranular and

intragranular matrix porosity delineated by blue-dye staining, illustrating connected pore networks critical for fluid storage and flow.

3.2 Geothermal Fluid Characterization

Approximately 197 wells have been documented in the Alaşehir geothermal field, including 58 reinjection wells prior to 2022, operated by different companies across several license areas (Stantec, 2020; Uytun, 2021; Mott et al., 2022). Cold groundwater shows elevated Ca–HCO_3 signatures, whereas most geothermal fluids fall within the Na-HCO_3 type, with others classified as mixed or Na-Cl waters, and major ions typically ordered as Na+K > Ca > Mg and HCO_3 > Cl > SO_4 (DSI, 2014; Rabet et al., 2017; Uytun, 2021). For this study, a synthetic geothermal brine was prepared to replicate the representative fluid chemistry of the Gediz Graben system, characterized by high bicarbonate (HCO_3^- ≈1,400–1,530 mg/L), elevated Na–K concentrations (Na ≈ 715–877 mg/L; K ≈ 80–95 mg/L), moderate chloride (Cl ≈ 245–330 mg/L), and significant dissolved silica (SiO_2 ≈ 285–310 mg/L). This artificial brine, reflecting median–mean values from field measurements, was used in all hydrothermal experiments to ensure realistic geochemical conditions during fluid–rock interaction tests. Beyond their dissolved ion signatures, the gas content of these fluids, particularly CO_2, also plays a critical role in reservoir behavior and operational sustainability. In the Menderes Massif, non-condensable gas (NCG) contents may reach 4–5%, largely due to CO_2 released from metamorphic decarbonation of carbonate-rich units (marbles and calc-schists). Similar high-temperature, high-CO_2 conditions characterize the Gediz Graben, including Alaşehir, where more than 96% of NCGs consist of CO_2. Numerous studies also support the related data on CO_2 ratios, geochemistry, and reservoir behavior in these systems (Akın, 2017; Akın et al., 2020; Aydın and Akın, 2019, 2021).

3.3 Hydrothermal Autoclave Experiments

Hydrothermal fluid–rock-CO_2 interaction tests were conducted using a 600 mL Parker Autoclave Engineers reactor at Durham University, operating safely within a 100 bar and a 70 °C temperature, which is nearly the same as the re-injection process in fields (Figure 3). A synthetic NaCl–Na_2CO_3 geothermal brine was reacted with 10 g of marble and schist samples for a minimum of seven days. Additionally, at Newcastle University, low-medium temperature dissolution experiments (25–50-110 °C) conducted using a thick-walled glass round-bottom flask established baseline carbonate kinetics, buffering capacity, and solubility thresholds, which guided the design and pressure–temperature selection for high-pressure runs.



Figure 3. Hydrothermal reactor setup for 70 °C and 100 bar experiment: a) control, monitoring system, b) protected reactor room, c) high-pressure autoclave, and CO_2 gas-supply unit.

At 70 °C and 100 bar, CO_2-injected autoclave tests were performed using carbonates with 200 mL of artificial brine and a 400 mL CO_2–N_2 headspace (approximately 50 bar each). PHREEQC simulations accurately replicated the exact brine chemistry and gas-phase composition. Saturation index (SI) calculations indicate that major carbonate phases (calcite, aragonite, dolomite) were mostly undersaturated (SI ≈ −1.8 to −1.0), though near-equilibrium conditions show that small pH or pCO_2 changes could rapidly trigger carbonate scaling (Figure 4). Quartz was at or slightly above equilibrium, whereas amorphous silica and chalcedony remained undersaturated, implying low silica-scaling risk at 70 °C but potential supersaturation during cooling. Sulfate minerals (gypsum, anhydrite) were strongly undersaturated, eliminating $CaSO_4$ scaling hazards. In contrast, $BaCO_3$ (witherite) was consistently supersaturated across all samples (SI ≈ +0.7 to +0.9), making it the dominant scaling risk under high-pCO_2 conditions. $SrCO_3$ and $BaSO_4$ remained undersaturated, indicating that Ba precipitation is controlled primarily by carbonate equilibria. Mg-bearing carbonates (magnesite, brucite) displayed negative SI values, while aluminosilicates (muscovite, illite, kaolinite) appeared thermodynamically oversaturated but are interpreted as kinetically inhibited during short-term runs.

The saturation index results obtained from the 70 °C and 100 bar CO_2-injected autoclave tests indicate that although major carbonate phases remained undersaturated overall, their proximity to equilibrium suggests strong sensitivity to small shifts in pH or pCO_2, conditions that could rapidly induce localized scaling. This thermodynamic framework aligns closely with the mineralogical evolution observed in the solid samples. Integrated XRF, SI, and SEM–EDX analyses collectively reveal how these bulk geochemical signals translate into a coherent sequence of microscale transformations during fluid–rock interaction under CO_2-charged conditions. Carbonate substrates initially undergo acid-driven dissolution, resulting in pervasive etching, dissolution pits, and terrace-like retreat that increase surface roughness and reactive surface area. As the interaction progresses and the fluid chemistry evolves toward supersaturation, these etched surfaces become nucleation sites for fine-grained secondary precipitates, including Ca–Mg phases and Fe-bearing minerals that are mobilized under high-pCO_2 conditions. With continued reaction, dense clusters of sub-10 µm rhombohedral Ca–Mg crystals, interpreted as magnesian calcite or early dolomite, progressively mantle the substrate, forming sealing layers that diminish porosity and permeability. This integrated dataset demonstrates that CO_2-rich geothermal fluids promote a tightly coupled cycle of dissolution followed by heterogeneous reprecipitation, resulting in stratified scaling layers that significantly impact injectivity, fluid flow pathways, and the long-term operational performance of geothermal reservoirs.

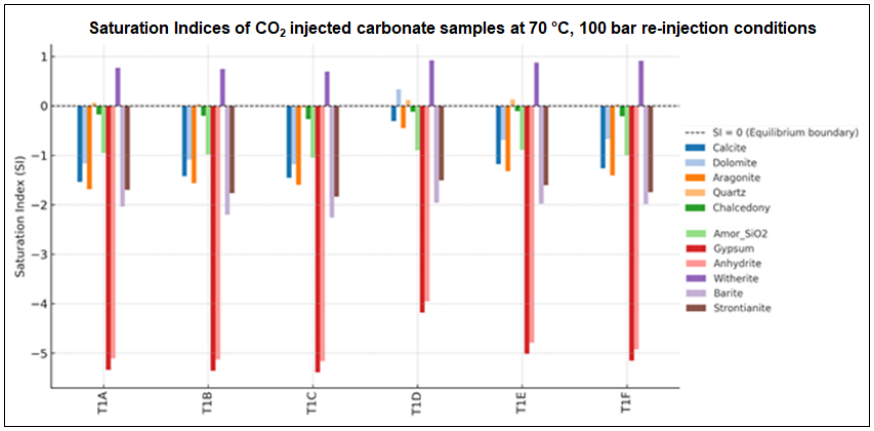


Figure 4. Saturation indices (SI) of selected mineral phases (carbonate, silica, sulfate, and Ba–Sr minerals) for six experimental brine samples with CO_2 injection at 70 °C and 100 bar.

4 DISCUSSION & CONCLUSION

This study demonstrates that CO_2 injection fundamentally alters mineral stability and fluid–rock interactions in carbonate- and schist-bearing geothermal systems. Elevated pCO_2 drives calcite, aragonite, and dolomite into undersaturation, suppressing classical carbonate scaling, while $BaCO_3$ (witherite) and Fe-oxides emerge as the dominant precipitation risks. Under these conditions, high CO_2, cold-water reinjection tends to dissolve carbonates in situ (reducing immediate scaling), but subsequent changes, such as reheating or degassing during mixing, can promote secondary carbonate or silica precipitation. Silica phases become increasingly undersaturated with temperature, indicating that silica scaling primarily occurs during cooling rather than under reservoir conditions. Hematite maintains very high saturation indices, consistent with Fe-rich surface precipitates, confirming its persistent operational relevance.

Notably, the SI trends indicate that CO_2-charged conditions at around 70 °C produce a distinct dissolution-dominated regime, whereas higher-temperature experiments, conducted without CO_2 injection, instead show the onset of thermally driven precipitation for Fe-bearing phases. Two thermal reaction windows were identified: strong carbonate dissolution and Ca–Mg mobilization near ~70 °C, and renewed carbonate and Fe-oxide precipitation at ≥110 °C. Injecting fluid significantly below reservoir temperature (e.g., at ~70 °C) led to pronounced carbonate dissolution; by contrast, higher injection temperatures (approaching ~100 °C) reduce thermal shock and keep the fluid closer to equilibrium, thereby limiting the extent of dissolution–precipitation cycles. These processes create significant injectivity risks in carbonate-rich units, whereas schist-bearing intervals show additional Mg–Si–Al release and secondary clay/oxide formation. These coupled chemical processes (dissolution and reprecipitation) ultimately lead to physical changes such as narrowed fracture apertures and reduced permeability, underscoring the need to carefully control reinjection temperature and chemistry. Maintaining reinjection temperatures above ~90–100 °C and monitoring Ba, Sr, and Fe are therefore key to minimizing scaling in CO_2-rich systems.

In addition to the chemical scaling behavior, the experimental results also demonstrate that schist-dominated intervals can retain meaningful porosity and permeability through fracture- and foliation-controlled pathways, reinforcing their critical role in sustaining reservoir performance. The experimentally derived datasets serve as essential inputs for calibrating reactive transport models, addressing a major limitation in current reservoir simulations that rely on generic parameters for carbonate systems. Integrating hydrothermal experiments with numerical modeling will clarify how reinjection temperature affects dissolution–precipitation cycles, injectivity, and the potential co-benefits of CO_2-based emission reduction. This combined petrographic, micro-CT, and geochemical workflow provides a robust foundation for upscaling petrophysical properties and improving reservoir-scale predictions in structurally complex metamorphic terrains such as the Menderes Massif. Technology transfer to the İzmir Institute of Technology further ensures long-term capability for industry-aligned research and sustainable geothermal resource management in Türkiye.

5 Acknowledgements

The work presented is a part of the project "Analytical and numerical modeling of chemical reactions and CO_2 re-injection processes due to physical changes in high temperature and pressure geothermal systems: A Case Study from Menderes Massif" and funded under the Scientific and Technological Research Council of Türkiye (TUBITAK)'s International Postdoctoral Research Fellowship Program-2219 (Project No:1059B192301691). X-Ray Computed Tomography analyses were conducted with the support of the Department of Archaeology at Durham University, whose assistance and access to facilities are gratefully acknowledged.

REFERENCES

Akbas, B., Akdeniz, N., Aksay, A., Altun, İ.E., Balcı, V., Bilginer, E., Bilgic, T. et al.: 1:1.250.000 scaled Geological Map of Turkey. General Directorate of Mineral Research and Exploration Publication, **2011**, Ankara-Turkey.

Akın, T.: CO_2 emissions from geothermal fields in the Büyük Menderes Graben, Western Turkey: Implications for monitoring and mitigation. Geothermics, **2017**, 65, 26–38. https://doi.org/10.1016/j.geothermics.2016.09.011

Akın, T., Korkmaz, E. D., Kılkış, Ş.: Greenhouse gas emissions from geothermal power plants in Turkey: Assessment and mitigation strategies. Renewable Energy, **2020**, 155, 1066–1078. https://doi.org/10.1016/j.renene.2020.03.143

Aydın, H., Akın, T.: Reservoir parameters and well interactions controlling CO_2 discharge in geothermal fields of the Büyük Menderes Graben, Turkey. Geothermics, **2019**, 80, 197–210. https://doi.org/10.1016/j.geothermics.2019.03.004

Aydın, H., Akın, T.: Geochemical monitoring of CO_2 and reservoir performance in geothermal systems of the Menderes Massif, Turkey. Journal of Volcanology and Geothermal Research, **2021**, 415, 107245. https://doi.org/10.1016/j.jvolgeores.2021.107245

Bozkurt, E., Sozbilir, H.: Tectonic evolution of the Gediz Graben: field evidence for an episodic, two-stage extension in western Turkey. Geological Magazine, **2004**, 141, 63–79.

Ciftci, N., Bozkurt, E.: Evolution of the Miocene sedimentary fill of the Gediz Graben, SW Turkey. Sedimentary Geology, **2009**, 216, 49-79.

DSI: Hydrogeological Study of the Gediz Watershed, Main Report. Devlet Su İşleri Genel Müdürlüğü-DSI (General Directorate of State Hydraulic Works) Eser Project & Engineering Inc., Ankara, **2014**, p. 553.

Emre, Ö., Duman, T.Y., Özalp, S. et al.: Active fault database of Turkey. Bull Earthquake Eng, **2018**, 16, 3229–3275. https://doi.org/10.1007/s10518-016-0041-2

İztan, H., Yazman, M.: Geology and hydrocarbon potential of the Alaşehir (Manisa) area, Western Turkey. IESCA, Int. Earth Sci. H. Yavuz HAKYEMEZ, Fikret GÖKTAŞ, Tevfik ERKAL 24 Congr. on Aegean Regions, **1990**, İzmir, 327-338.

Kocyigit, A., Yusufoglu, H., Bozkurt, E.: Evidence from the Gediz graben for episodic two-stage extension in western Turkey. Journal of the Geological Society, London, **1999**, 156, 605-616.

Mott, A., Baba, A., Mosleh, A.M. Ökten, H.E., Babaei, M., Gören, A.Y., Feng, C., Recepoğlu, Y.K., Uzelli, T., et al.: Boron in geothermal energy: Sources, environmental impacts, and management in geothermal fluid. Renewable and Sustainable Energy Reviews, **2022**, 167, 112825. https://doi.org/10.1016/j.rser.2022.112825

Rabet, R.S., Simsek, C., Baba, A., Murathan, A.: Blowout mechanism of Alasehir (Turkey) geothermal field and its effects on groundwater chemistry. Environmental Earth Sciences, **2017**, 76(1). doi:10.1007/s12665-016-6334-6

Sozbilir, H.: "Extensional Tectonics and the Geometry of Related Macroscopic Structures: Field Evidence from the Gediz Detachment, Western Turkey," Turkish Journal of Earth Sciences, **2001**, Vol. 10: No. 2, Article 1. Available at: https://journals.tubitak.gov.tr/earth/vol10/iss2/1

Stantec: Cumulative impact assessment report of "Cumulative Impact Assessment of Geothermal Resources in Turkey". European Bank for Reconstruction and Development, July, **2020**.

Uytun, H.: Relation between induced seismicity and geothermal systems: A case study from the Gediz graben, Western Anatolia, Turkey. Master's Thesis, Dokuz Eylül University, Department of Geological Engineering, **2021**, Izmir, Turkey, p 90.